https://doi.org/10.5194/egusphere-2025-5486
Preprint. Discussion started: 8 January 2026

Brief Communication: Inferring Glacier Equilibrium Line Altitudes in Central Europe with FROST

Oskar Herrmann[1], Veena Prasad[1], Anna Zöller[1], Alexander R. Groos[1], Samuel Cook[1], Christian Sommer[1], and Johannes J. Fürst[1]

[1]Institute of Geography, Friedrich-Alexander-Universität Erlangen-Nürnberg, Germany

Correspondence: Oskar Herrmann (oskar.herrmann@fau.de)

Abstract. Glaciers in Central Europe are projected to almost disappear by 2100. To improve projections, glacier models must be calibrated to match observations. Using the open-source `Framework for assimilating Remote-sensing Observations for Surface mass balance Tuning (FROST)`, we infer equilibrium-line altitudes (ELAs) and surface mass balance parameters for 409 Alpine glaciers during 2000–2019 through an Ensemble Kalman Filter. The method combines an elevation-dependent surface mass balance model with ice dynamics from Instructed Glacier Model (IGM). Validation against in-situ mass balance and end-of-summer snowline data (correlations of 0.76 and 0.62) shows that FROST enables satellite-based regional estimates of glacier equilibrium conditions.

1 Introduction

Mountain glaciers are losing mass worldwide in response to anthropogenic climate change (The GlaMBIE Team, 2025) and are currently among the largest contributors to sea-level rise, comparable to the combined meltwater from Greenland and Antarctica (Slater et al., 2021). In the European Alps, roughly 4,000 glaciers were cataloged around the year 2000 (RGI Consortium, 2023), but most are projected to disappear by the end of the century due to climate change (Zekollari et al., 2025). At present, these glaciers are vital for local hydrology (Koboltschnig and Schöner, 2011), hydroelectric power (Schaefli et al., 2019), and hazard management (Haeberli et al., 2017). In Switzerland alone, around 200,000 people live in areas directly influenced by glacier meltwater, glacial lakes, or periglacial processes (Huss et al., 2017). Their retreat has already shifted seasonal runoff patterns (Huss and Hock, 2018), increased slope instability (Deline et al., 2015; Islam et al., 2025), and led to the formation of new proglacial lakes. Underscoring the urgency to better understand their evolution and associated risks in this densely populated region.

Accurate modeling of glacier evolution requires a realistic representation of both the surface mass balance and the ice dynamics. The Surface Mass Balance (SMB) quantifies all processes of surface accumulation and melt. Existing SMB models range from simple temperature-index approaches to physically based energy balance models (Hock et al., 2019). Since the publication of Hugonnet et al. (2021), SMB model calibration has often aimed to match a scalar geodetic mass balance (Maussion et al., 2019; Rounce et al., 2023). However, theses approaches strongly reduces the spatial information contained in modern

https://doi.org/10.5194/egusphere-2025-5486
Preprint. Discussion started: 8 January 2026

remote-sensing products, such as elevation change or velocity fields (Hugonnet et al., 2021; Sommer et al., 2020). Efficient methods are therefore needed to assimilate such spatially distributed datasets directly into the calibration process.

The representation of ice dynamics is equally essential for glacier modeling. Flow-line models remain widely used due to their computational efficiency and ability to reduce glacier geometry to its key dimensions: length, thickness, and surface elevation along a central flow line (Maussion et al., 2019; Rounce et al., 2023). With the recent development of the IGM (Jouvet and Cordonnier, 2023), it has become feasible to simulate three-dimensional glacier flow at reasonable computational cost. IGM also enables the inversion for ice thickness and basal sliding, which are essential for constraining the internal glacier structure and basal conditions. While satellite-based velocity products are increasingly available (Friedl et al., 2021; Millan et al., 2022), they are rarely used for model calibration in large-scale glacier modeling frameworks.

Ensemble-based data assimilation methods such as the Ensemble Kalman Filter (EnKF) (Evensen, 1994) have gained traction in glaciology for parameter and state estimation. The EnKF offers a derivative-free alternative to adjoint-based methods (Higdon et al., 2012; Iglesias et al., 2013), which, in contrast, require gradient computations and full access to the model internals . Applications include ensemble transform Kalman filter-based parameter estimation (Bonan et al., 2014) and assimilation of surface observations in ice sheet models (Gillet-Chaulet, 2020). Variational approaches, such as adjoint methods (Goldberg and Heimbach, 2013), remain powerful but computationally demanding. Recent work by Knudsen et al. (2024) and Herrmann et al. (2025) demonstrated the potential of EnKF for calibrating SMB parameters in a synthetic glacier setting.

Building on the `Framework for assimilating Remote-sensing Observations for Surface mass balance Tuning (FROST)` introduced by Herrmann et al. (2025), we apply it to elevation-change observations from 2000–2019 for the 409 glaciers in Central Europe which exceeded 1 km^2 in 2000. The framework combines the three-dimensional glacier evolution model IGM with an EnKF to iteratively calibrate elevation-dependent SMB parameters and quantify their uncertainties. This approach enables the calibration of glacier-specific Equilibrium Line Altitudes (ELAs) and mass-balance gradients, where the ELA represents the climatic boundary between accumulation and ablation and the gradients describe how these processes vary with elevation. We focus on long-term spatial patterns of accumulation and ablation, as multi-year elevation-change observations provide more robust constraints. The inferred ELAs are validated against independent end-of-summer snow line altitude (EoS SLA) derived from remote sensing and in-situ SMB measurements from Glacier Monitoring Switzerland (GLAMOS), demonstrating that FROST provides consistent, observation-constrained estimates of glacier equilibrium conditions across the European Alps.

2 Data and Method

The FROST calibration pipeline (Herrmann et al., 2025) integrates the IGM (Jouvet and Cordonnier, 2023)) with the EnKF (Evensen, 1994) to estimate glacier-specific SMB parameters. The SMB model used here is an elevation-dependent piecewise-linear function and does not take climate variables as input (Eq. 1).

https://doi.org/10.5194/egusphere-2025-5486
Preprint. Discussion started: 8 January 2026

$$SMB(z) = \begin{cases} \beta_{acc} \cdot (z - z_{ELA}) & \text{if } z > z_{ELA}, \\ \beta_{abl} \cdot (z - z_{ELA}) & \text{otherwise.} \end{cases} \quad (1)$$

where z denotes the elevation of the glacier surface, z_{ELA} the ELA, β_{acc} and β_{abl} the accumulation and the ablation gradient respectively. The EnKF is used to iteratively update SMB parameters by minimizing the misfit between modeled and observed elevation change. It is worth noting that IGM assumes a constant ice density of 910 kg m^{-3}. A detailed description of the `FROST` methodology is provided in Herrmann et al. (2025).

The framework utilizes Open Global Glacier Model (OGGM)-shop to download, align, and pre-process surface elevation (Crippen et al., 2016), surface velocity (Millan et al., 2022), and glacier outlines from the RGI Consortium (2023). The IGM inversion for thickness and sliding coefficient includes optimization parameters, which is manually tuned based on the examples provided in the IGM repository, aiming to balance the tendency to overestimate thickness for small glaciers against underestimation for large glaciers. We use elevation-change observations from Hugonnet et al. (2021), which provide globally gridded glacier-wide elevation change rates between 2000 and 2019. These rates are added to the NASADEM 2000 elevation data to reconstruct the 2019 surface topography, with the associated uncertainties in elevation change propagated into the 2019 elevation uncertainty. The method can be easily extended to other regions because we chose this global dataset.

For validation, we compare the calibrated SMB parameters with glaciological measurements provided by GLAMOS. Multi-year mean ELA values and SMB gradients are derived from the elevation-binned mass balance product. As these measurements are not used in the calibration process, they serve as an independent reference for assessing the physical plausibility of our inferred parameters. We select glaciers with more than five years of ELA data to ensure a stable, representative value for the 20-year period.

To further evaluate the inferred ELAs, we compare them to EoS SLAs. The snow lines of glaciers in the European Alps are estimated using optical remote sensing images from the Landsat and Sentinel-2 satellite missions. We distinguish between areas of bare glacier ice and snow cover by automatically estimating intensity thresholds from infrared reflectance histograms based on Otsu's method Otsu (1979). Thereby, the glacier area covered by snow is identified due to the relatively high near- (NIR) and shortwave-infrared (SWIR) reflectance of snow compared to bare ice or debris Hall et al. (1987). The date-specific snow line altitude is then derived by masking the surface elevations of the NASADEM with the pixels of each satellite image that are classified as snow. For each glacier and year, the EoS SLA is defined as the highest transient snowline observed during the late ablation season (15 August–30 September). Estimates based on fewer than three suitable satellite scenes were subjected to outlier detection. For glaciers with at least ten valid years, values deviating by more than ± 3 standard deviations from the glacier-specific mean were removed. For glaciers with fewer than ten valid years, an additional physical threshold was applied, excluding EoS SLAs differing by more than 400 m from the mean glacier elevation (RGI v7). The mean EoS SLA for 2000–2019 was then computed from all non-flagged years. As EoS SLA serves as a proxy for annual ELA, the dataset provides an independent benchmark for evaluating the calibrated ELA values.

https://doi.org/10.5194/egusphere-2025-5486
Preprint. Discussion started: 8 January 2026

We restrict the comparison to glaciers larger than 1 km^2, and assess agreement using the Pearson correlation coefficient (Eq. 2) and mean absolute error.

$$r = \frac{\sum_{i=1}^{n}(x_i - \bar{x})(y_i - \bar{y})}{\sqrt{\sum_{i=1}^{n}(x_i - \bar{x})^2}\sqrt{\sum_{i=1}^{n}(y_i - \bar{y})^2}} \tag{2}$$

where y_i are the observed values, x_i the corresponding calibrated or modeled values, $\bar{x}$ and $\bar{y}$ their respective means, and n the number of paired samples.

3 Results

We applied the workflow described in Section 2 to the glaciers in Central Europe and calibrated glacier specific ELA for this region. Here, we summarize regional patterns, validation against the GLAMOS dataset, and compare with EoS SLA extracted from optical imagery.

3.1 Regional equilibrium line altitude distribution

Our calibration results yield an ELA range of from 2540 to 3540 m a.s.l. for the Alps in the period 2000-2019, with a mean of 3158 m a.s.l. and a standard deviation of 157 m. The spatial distribution of modeled ELAs reflects the main climatic gradients across the Alps: lower values occur along the northern and western flanks, while higher values dominate in the higher inner Alps (Fig. 1). While ELAs correlates with mean glacier elevation, no other systematic relation with glacier size or aspect emerges at the scale of the entire Alps (see Supplementary Material S1), although in some subregions the observed spread is likely influenced by hypsometry and exposure. Local deviations can further arise from shading, debris cover, and other surface or topographic effects.

3.2 Validation with end-of-summer snow line altitude

The close match between modeled and observed elevation change demonstrates that the filter effectively combines observations and model output (Fig. 2a). Figure 2b shows that the ELA correlation with EoS SLA-based ELA proxies exhibit a similar spatial pattern, as indicated by a Pearson correlation of 0.62. The mean absolute error of 217 m is largely driven by a bias of 190 m. This bias can be attributed to a systematic underestimation of the EoS SLA, since the underlying imagery typically does not capture the day of maximum EoS SLA retreat. After applying a bias correction (subtracting the bias from each calibrated ELA so that both sets have the same mean) the mean absolute error decreases to 129 m.

3.3 Validation against glaciological observations

The modeled and observed ELAs cluster around the diagonal, indicating a consistent agreement across a range of different glaciers (Fig. 3a). Only the Grosser Aletschgletscher has a much higher calibrated (3399 m a.s.l.) than observed (3034 m a.s.l.) ELA. Modeled and observed gradients show however, less correlation (Fig. 3b,c). Reasons are diverse and include variations

https://doi.org/10.5194/egusphere-2025-5486
Preprint. Discussion started: 8 January 2026

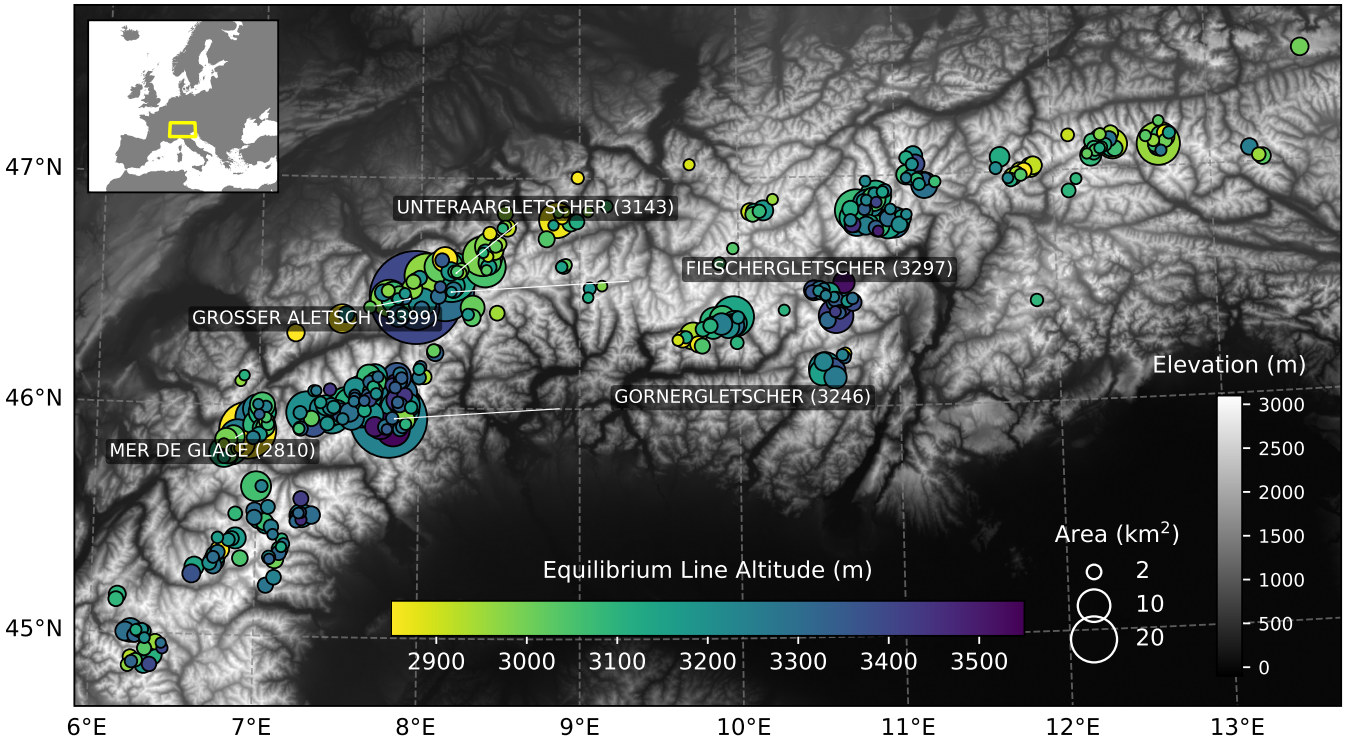

Figure 1. Coloured circles show the mean ELA of glaciers in the European Alps for the period 2000–2019, using FROST. The background topography is taken from © EuroGeographics.

in ablation gradients driven by local ice-flow dynamics, as well as poorly constrained accumulation gradients, since many glaciers in this region have only small or no-longer-extant accumulation areas. Consequently, the accumulation gradient has little influence on the overall elevation change. Reasons for the deviation of the ablation gradients are discussed in Section 4.

The correlation between the Hugonnet et al. (2021) elevation change dataset (used for calibration) and GLAMOS mass balance observations (used for evaluation) supports the comparison of calibrated SMB parameters against parameters derived from GLAMOS (Fig. 3e). We acknowledge that volume change and mass change are not identical, but their strong correlation allows deviations to help explain mismatches in the calibrated parameters. The agreement of the ice-dynamic parameters underlying the SMB calibration suggests that ice-dynamic constraints are broadly consistent (Fig. 3f-h). However, this agreement reflects similarity in mean values, while spatial distributions can differ substantially. It should also be noted that thickness measurements are sparse, and the modeled thickness can deviate from reasonable values in areas without observations.

4 Discussion

Achieving consistency between observed and modeled glacier velocity and thickness typically requires glacier-specific tuning of the IGM inversion parameters. Applying a single parameter set to all 409 glaciers inevitably stretches the inversion's ca-

https://doi.org/10.5194/egusphere-2025-5486
Preprint. Discussion started: 8 January 2026

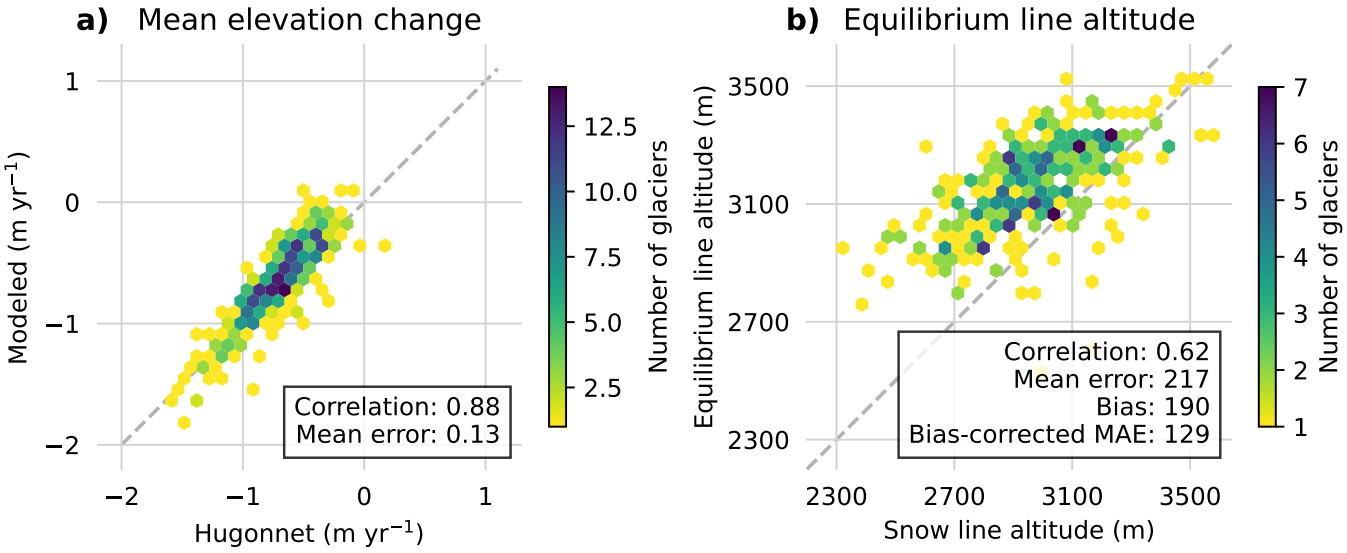

Figure 2. Comparison with observed elevation change and EoS SLA. Panel a shows modeled and observed elevation change, and panel b shows modeled ELA and EoS SLA. Both panels use hexagon density plots, where color indicates the number of glaciers per bin. Pearson correlation coefficients and mean absolute errors are given in each panel.

pabilities, as no systematic procedure for automated tuning currently exists and manual adjustment for each glacier is not feasible. After extensive testing, we adopted a compromise parameter set for IGM 3.0.0 (available at https://github.com/FAU-glacier-systems/FROST/tree/hydra), balancing the tendency to overestimate thickness in small glaciers against underestimation in large ones. The Grosser Aletschgletscher is particularly affected, as it is by far the largest glacier in the GLAMOS sample with an area of 81 km^2 (the second largest, Glacier de Corbassière, covers 16 km^2). For such large glaciers, the current inversion performs less accurately, and an adapted parameter set would yield more realistic ice-dynamic parameters. However, to maintain a broadly applicable workflow, we use a uniform parameter set. A more adaptive method would certainly improve the ice-flow parameters and, in turn, the calibration of the SMB parameters.

Inaccuracies in the input datasets can propagate through the calibration. Elevation-change products such as Hugonnet et al. (2021) rely on temporal aggregation and may exhibit regional biases. We also observed unrealistically high velocity patches in the surface velocity fields from Millan et al. (2022) for several glaciers (Plaine Morte, Glacier de Tsanfleuron, and Glacier du Gietro). Such artifacts can introduce inconsistencies between modeled and actual ice dynamics and may partly explain the stronger calibrated ablation gradients, as excessive ice transport toward the glacier front requires higher ablation rates to match the observed elevation changes.

The simplification of the SMB models to the elevation only neglects the horizontal variability. Although SMB and elevation change are primarily governed by elevation, lateral differences are not represented and can be significant, particularly in branching glaciers where flow and mass balance vary across the same elevation.

https://doi.org/10.5194/egusphere-2025-5486
Preprint. Discussion started: 8 January 2026

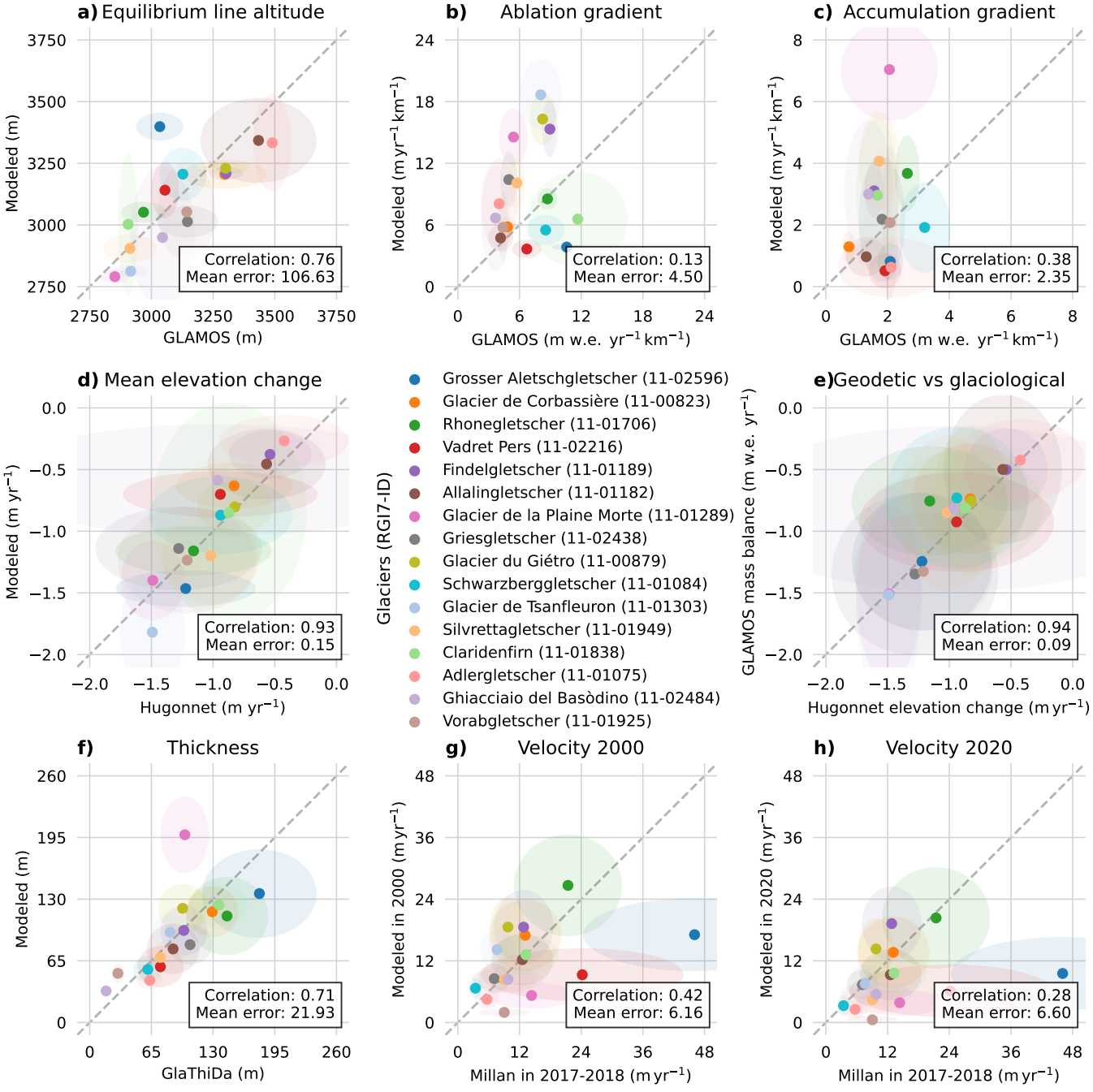

Figure 3. Validation against glaciological observations. Sub-panels show (a) ELA, (b) ablation gradient, (c) accumulation gradient, (d) mean elevation change used as EnKF target, and (e–h) ice-dynamic parameters and product consistency. Pearson correlation coefficients and mean absolute errors are given in each panel.

https://doi.org/10.5194/egusphere-2025-5486
Preprint. Discussion started: 8 January 2026

Validation against EoS SLA-based proxies and GLAMOS mass balance observations may show deviations that do not necessarily indicate calibration errors, but rather reflect that these products represent related, yet not identical, quantities. EoS SLA data are spatially aggregated and sensitive to threshold definitions, while GLAMOS mass balance data rely on interpolation between sparse stake measurements and may not capture localized variability. Despite these limitations, the regional agreement demonstrates that the workflow captures the main climatic and topographic controls on ELA across the Alps.

Overall, the analysis highlights that the FROST framework reproduces key climatic and geometric dependencies of glacier mass balance, yet remains sensitive to initialization and data quality. Future developments should first address the initialization through improved inversion strategies and, once a stable initialization is achieved, focus on integrating transient data assimilation methods to assimilate observations at their acquisition time.

5 Conclusion

We present a regional workflow to calibrate SMB parameters representing the period 2000–2019 including estimates of ELAs for all glaciers larger than 1 km^2 across the European Alps in the year 2000. The approach integrates glacier modeling within an EnKF framework and is evaluated against independent observations from GLAMOS and EoS SLA derived from optical satellite imagery.

(1) The workflow successfully reproduces large-scale ELA patterns across the Alps, showing good agreement with glaciological observations and consistent relationships to EoS SLA. This demonstrates that the approach captures the main climatic and topographic controls on glacier mass balance at a regional scale.

(2) Deviations in ablation and accumulation gradients reveal remaining limitations. The simplified elevation-based SMB model and uniform inversion parameters currently limit `FROST`'s performance.

(3) Inaccuracies in input data affect the calibration. Global velocity products can locally overestimate motion on small glaciers, introducing inconsistencies and partly explaining stronger calibrated ablation gradients.

Overall, the Python-based, fully open-source `FROST` framework demonstrates strong potential for calibrating glacier models with remotely sensed observations. Future developments should aim to improve the IGM inversion through glacier-specific or adaptive parameter tuning and to better account for initialization-related ice-dynamic effects. The framework is open to other data sources of elevation change or ice velocity. Combining multiple data-sources is a great potential of the framework reducing uncertainties of observations. With these refinements, `FROST` will enable more robust assimilation of time-dependent observations for regional glacier monitoring and projection.

Code availability. The workflow presented in this study is implemented in the open-source `FROST` framework, available under a permissive license at https://github.com/FAU-glacier-systems/FROST. The underlying ice-flow inversion uses IGM version 3.0.0 (Jouvet and Cordon-

https://doi.org/10.5194/egusphere-2025-5486
Preprint. Discussion started: 8 January 2026

nier, 2023), which is also publicly available at https://github.com/jouvetg/igm. All scripts required to reproduce the regional calibration experiments and figures are archived with the publication (see Supplement).

Data availability. The Hugonnet et al. (2021) elevation-change dataset is publicly available from https://doi.org/10.6096/13. Glacier outlines are taken from RGI v7.0 (RGI Consortium, 2023), accessible at https://www.glims.org/RGI/. Glacier-specific reference mass-balance data are provided by GLAMOS (GLAMOS - Glacier Monitoring Switzerland, 2023), available at https://doi.org/10.18750/massbalance.2020.r2021. All processed ELA and SMB parameter outputs generated in this study are archived together with the publication (see Supplement).

Author contributions. OH designed the study, performed the model runs, and analyzed the results. VP, AZ, and SC contributed through discussions that improved the understanding and application of the glacier model and provided input on the workflow. CS contributed expertise on remote sensing. ARG provided expertise on the interpretation of glaciological measurements and surface mass balance properties. JJF assisted with model implementation, supervised the project, and contributed to the conceptual framing. All authors discussed the results and contributed to the writing of the manuscript.

Competing interests. Johannes J. Fürst is a member of the editorial board of TC.

Acknowledgements. OH, VP, ARG, and JJF received primary funding from the European Union's Horizon 2020 research and innovation programme via the European Research Council (ERC) as a Starting Grant (FRAGILE project) under grant agreement No. 948290. AZ acknowledges support from the Response project (DFG Individual Research Grant No. 495516510). SC acknowledges funding from the Elitenetzwerk Bayern through the DeLIGHT project. The processing of data on snow-line elevation based on remote-sensing images was financially supported by the Dr. Hertha & Helmut Schmauser Research Foundation as part of the funded proposal *"Automated measurement of seasonal snow cover on glaciers using time-series analysis of optical satellite data in Google Earth Engine."*

This research was supported by the M^{3}OCCA graduate school and by computational resources provided by the NHR@FAU. We thank the developers of OGGM and IGM for providing the modeling tools on which this work builds. We also thank GLAMOS for providing reference mass-balance data and the RGI consortium for making glacier outlines openly available. We acknowledge Hugonnet et al. (2021) and Millan et al. (2022) for making elevation-change and ice-velocity data accessible and are especially grateful to Romain Hugonnet for guidance on the interpretation of observed elevation-change uncertainties.

Parts of the manuscript were refined using ChatGPT (OpenAI, version October 2025) to improve clarity and wording. All scientific content and interpretations were developed and verified by the authors.

https://doi.org/10.5194/egusphere-2025-5486
Preprint. Discussion started: 8 January 2026

References

Bonan, B., Nodet, M., Ritz, C., and Peyaud, V.: An ETKF approach for initial state and parameter estimation in ice sheet modelling, Nonlinear Processes in Geophysics, 21, 569–582, https://doi.org/10.5194/npg-21-569-2014, 2014.

Crippen, R., Buckley, S., Agram, P., Belz, E., Gurrola, E., Hensley, S., Kobrick, M., Lavalle, M., Martin, J., Neumann, M., Nguyen, Q., Rosen, P., Shimada, J., Simard, M., and Tung, W.: NASADEM GLOBAL ELEVATION MODEL: METHODS AND PROGRESS, The International Archives of the Photogrammetry, Remote Sensing and Spatial Information Sciences, XLI-B4, 125–128, https://doi.org/10.5194/isprs-archives-XLI-B4-125-2016, 2016.

Deline, P., Gruber, S., Delaloye, R., Fischer, L., Geertsema, M., Giardino, M., Hasler, A., Kirkbride, M., Krautblatter, M., Magnin, F., McColl, S., Ravanel, L., and Schoeneich, P.: Chapter 15 - Ice Loss and Slope Stability in High-Mountain Regions, in: Snow and Ice-Related Hazards, Risks, and Disasters, edited by Shroder, J. F., Haeberli, W., and Whiteman, C., Hazards and Disasters Series, pp. 521–561, Academic Press, Boston, ISBN 978-0-12-394849-6, https://doi.org/10.1016/B978-0-12-394849-6.00015-9, 2015.

Evensen, G.: Sequential data assimilation with a nonlinear quasi-geostrophic model using Monte Carlo methods to forecast error statistics, Journal of Geophysical Research: Oceans, 99, 10 143–10 162, https://doi.org/10.1029/94JC00572, 1994.

Friedl, P., Seehaus, T., and Braun, M.: Global time series and temporal mosaics of glacier surface velocities derived from Sentinel-1 data, Earth System Science Data, 13, 4653–4675, https://doi.org/10.5194/essd-13-4653-2021, 2021.

Gillet-Chaulet, F.: Assimilation of surface observations in a transient marine ice sheet model using an ensemble Kalman filter, The Cryosphere, 14, 811–832, https://doi.org/10.5194/tc-14-811-2020, 2020.

GLAMOS - Glacier Monitoring Switzerland: Swiss Glacier Volume Change (release 2023), https://doi.org/10.18750/VOLUMECHANGE.2023.R2023, 2023.

Goldberg, D. N. and Heimbach, P.: Parameter and state estimation with a time-dependent adjoint marine ice sheet model, The Cryosphere, 7, 1659–1678, https://doi.org/10.5194/tc-7-1659-2013, 2013.

Haeberli, W., Alean, J.-C., Müller, P., and Funk, M.: Assessing Risks from Glacier Hazards in High Mountain Regions: Some Experiences in the Swiss Alps, Annals of Glaciology, 13, 96–102, https://doi.org/10.3189/S0260305500007709, 2017.

Hall, D. K., Ormsby, J. P., Bindschadler, R. A., and Siddalingaiah, H.: Characterization of Snow and Ice Reflectance Zones On Glaciers Using Landsat Thematic Mapper Data, Annals of Glaciology, 9, 104–108, https://doi.org/10.3189/S0260305500000471, 1987.

Herrmann, O., Groos, A. R., Tabone, I., Jouvet, G., and Fürst, J. J.: A Kalman filter-based framework for assimilating remote sensing observations into a surface mass balance model, Annals of Glaciology, 66, e23, https://doi.org/10.1017/aog.2025.10020, 2025.

Higdon, D., Pratola, M., Gattiker, J., Lawrence, E., Habib, S., Heitmann, K., Price, S., Jackson, C., and Tobis, M.: Computer Model Calibration using the Ensemble Kalman Filter, http://arxiv.org/abs/1204.3547, arXiv:1204.3547, 2012.

Hock, R., Bliss, A., Marzeion, B., Giesen, R. H., Hirabayashi, Y., Huss, M., Radić, V., and Slangen, A. B. A.: GlacierMIP – A model intercomparison of global-scale glacier mass-balance models and projections, Journal of Glaciology, 65, 453–467, https://doi.org/10.1017/jog.2019.22, 2019.

Hugonnet, R., McNabb, R., Berthier, E., Menounos, B., Nuth, C., Girod, L., Farinotti, D., Huss, M., Dussaillant, I., Brun, F., and Kääb, A.: Accelerated global glacier mass loss in the early twenty-first century, Nature, 592, 726–731, https://doi.org/10.1038/s41586-021-03436-z, 2021.

Huss, M. and Hock, R.: Global-scale hydrological response to future glacier mass loss, Nature Climate Change, 8, 135–140, https://doi.org/10.1038/s41558-017-0049-x, 2018.

https://doi.org/10.5194/egusphere-2025-5486
Preprint. Discussion started: 8 January 2026

Huss, M., Bookhagen, B., Huggel, C., Jacobsen, D., Bradley, R., Clague, J., Vuille, M., Buytaert, W., Cayan, D., Greenwood, G., Mark, B., Milner, A., Weingartner, R., and Winder, M.: Toward mountains without permanent snow and ice, Earth's Future, 5, 418–435, https://doi.org/10.1002/2016EF000514, _eprint: https://agupubs.onlinelibrary.wiley.com/doi/pdf/10.1002/2016EF000514, 2017.

Iglesias, M. A., Law, K. J. H., and Stuart, A. M.: Ensemble Kalman methods for inverse problems, Inverse Problems, 29, 045 001, https://doi.org/10.1088/0266-5611/29/4/045001, publisher: IOP Publishing, 2013.

Islam, N., Carrivick, J. L., Coulthard, T., Westoby, M., Dunning, S., and Gindraux, S.: A growing threat of multi-hazard cascades highlighted by the Birch Glacier collapse and Blatten landslide in the Swiss Alps, Geology Today, 41, 200–205, https://doi.org/10.1111/gto.12526, _eprint: https://onlinelibrary.wiley.com/doi/pdf/10.1111/gto.12526, 2025.

Jouvet, G. and Cordonnier, G.: Ice-flow model emulator based on physics-informed deep learning, Journal of Glaciology, 69, 1941–1955, https://doi.org/10.1017/jog.2023.73, 2023.

Knudsen, L., Park-Kaufmann, H., Corcoran, E., Robel, A., and Mayo, T.: The Potential of the Ensemble Kalman Filter to Improve Glacier Modeling, La Matematica, 3, 1085–1102, https://doi.org/10.1007/s44007-024-00116-y, 2024.

Koboltschnig, G. R. and Schöner, W.: The relevance of glacier melt in the water cycle of the Alps: the example of Austria, Hydrology and Earth System Sciences, 15, 2039–2048, https://doi.org/10.5194/hess-15-2039-2011, publisher: Copernicus GmbH, 2011.

Maussion, F., Butenko, A., Champollion, N., Dusch, M., Eis, J., Fourteau, K., Gregor, P., Jarosch, A. H., Landmann, J., Oesterle, F., Recinos, B., Rothenpieler, T., Vlug, A., Wild, C. T., and Marzeion, B.: The Open Global Glacier Model (OGGM) v1.1, Geoscientific Model Development, 12, 909–931, https://doi.org/10.5194/gmd-12-909-2019, publisher: Copernicus GmbH, 2019.

Millan, R., Mouginot, J., Rabatel, A., and Morlighem, M.: Ice velocity and thickness of the world's glaciers, Nature Geoscience, 15, 124–129, https://doi.org/10.1038/s41561-021-00885-z, 2022.

Otsu, N.: A Threshold Selection Method from Gray-Level Histograms, IEEE Transactions on Systems, Man, and Cybernetics, 9, 62–66, https://doi.org/10.1109/TSMC.1979.4310076, 1979.

RGI Consortium: Randolph Glacier Inventory - A Dataset of Global Glacier Outlines. (NSIDC-0770, Version 7). [Data Set]. Boulder, Colorado USA. National Snow and Ice Data Center., https://doi.org/10.5067/F6JMOVY5NAVZ, 2023.

Rounce, D. R., Hock, R., Maussion, F., Hugonnet, R., Kochtitzky, W., Huss, M., Berthier, E., Brinkerhoff, D., Compagno, L., Copland, L., Farinotti, D., Menounos, B., and McNabb, R. W.: Global glacier change in the 21st century: Every increase in temperature matters, Science, 379, 78–83, https://doi.org/10.1126/science.abo1324, 2023.

Schaefli, B., Manso, P., Fischer, M., Huss, M., and Farinotti, D.: The role of glacier retreat for Swiss hydropower production, Renewable Energy, 132, 615–627, https://doi.org/10.1016/j.renene.2018.07.104, 2019.

Slater, T., Lawrence, I. R., Otosaka, I. N., Shepherd, A., Gourmelen, N., Jakob, L., Tepes, P., Gilbert, L., and Nienow, P.: Review article: Earth's ice imbalance, The Cryosphere, 15, 233–246, https://doi.org/10.5194/tc-15-233-2021, 2021.

Sommer, C., Malz, P., Seehaus, T. C., Lippl, S., Zemp, M., and Braun, M. H.: Rapid glacier retreat and downwasting throughout the European Alps in the early 21st century, Nature Communications, 11, 3209, https://doi.org/10.1038/s41467-020-16818-0, publisher: Nature Publishing Group, 2020.

The GlaMBIE Team: Community estimate of global glacier mass changes from 2000 to 2023, Nature, 639, 382–388, https://doi.org/10.1038/s41586-024-08545-z, 2025.

Zekollari, H., Schuster, L., Maussion, F., Hock, R., Marzeion, B., Rounce, D. R., Compagno, L., Fujita, K., Huss, M., James, M., Kraaijenbrink, P. D. A., Lipscomb, W. H., Minallah, S., Oberrauch, M., Van Tricht, L., Champollion, N., Edwards, T., Farinotti, D., Im-

https://doi.org/10.5194/egusphere-2025-5486
Preprint. Discussion started: 8 January 2026

merzeel, W., Leguy, G., and Sakai, A.: Glacier preservation doubled by limiting warming to 1.5°C versus 2.7°C, Science, 388, 979–983, https://doi.org/10.1126/science.adu4675, publisher: American Association for the Advancement of Science, 2025.